Fuel 133 (2014) 263–269

Contents lists available at ScienceDirect

Fuel

journal homepage: www.elsevier.com/locate/fuel

The co-benefit of elemental mercury oxidation and slip ammonia abatement with SCR-Plus catalysts

Wanmiao Chen, Yongpeng Ma, Naiqiang Yan *, Zan Qu *, Shijian Yang, Jiangkun Xie, Yongfu Guo, Lingang Hu, Jinping Jia

School of Environmental Science and Engineering, Shanghai Jiao Tong University, Shanghai 200240, China

HIGHLIGHTS

- The concept of SCR-Plus for catalytic conversion of Hg^0 and slip NH_3 was put forward.
- The effect of doping Ru over SCR on NO_x reduction was investigated.
- The Mo–Ru/SCR displayed excellent activity of Hg^0 oxidation and NH_3 decomposition.
- The mechanism of Hg^0 oxidation and NH_3 decomposition was discussed.

GRAPHICAL ABSTRACT

The conception of the SCR-Plus and its integration with the typical SCR catalyst.

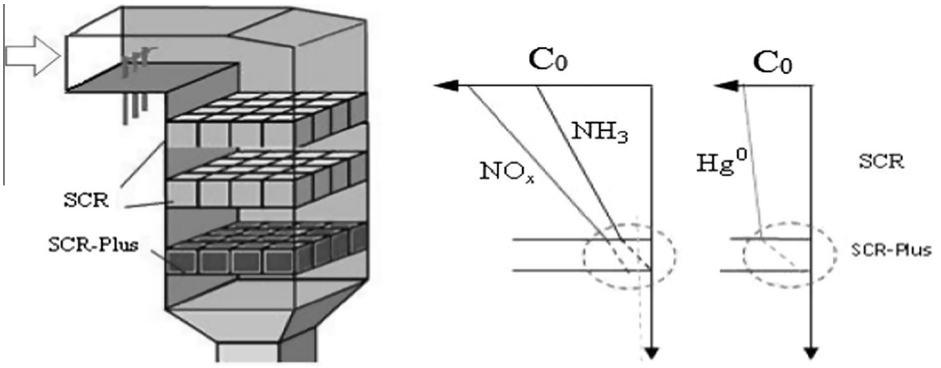

ARTICLE INFO

Article history:
Received 7 March 2014
Received in revised form 17 April 2014
Accepted 29 April 2014
Available online 10 May 2014

Keywords:
SCR
Ru
Slip ammonia
Elemental mercury
Deacon reaction

ABSTRACT

To enhance the co-benefits of elemental mercury (Hg^0) oxidation across the selective catalytic reduction (NH_3–SCR) units and to minimize slip ammonia (unreacted reductant) from flue gases, the conception of SCR-Plus was put forwarded and the catalysts were investigated. The SCR-Plus catalysts were prepared by modifying the conventional SCR catalyst with molybdenum (Mo) and ruthenium (Ru) to meet such purposes at relatively high space velocity. It was found the doping of Mo to Ru/SCR catalyst could significantly reduce the demand content of Ru, and the catalyst exhibited outstanding catalytic activity for Hg^0 oxidation and more tolerant to the inhibition of SO_2 and ammonia, respectively. Meanwhile, the cooperation of Mo and Ru in the SCR catalyst facilitated the abatement of slip ammonia. The Hg^0 removal efficiency of the Mo/Ru–SCR catalyst was greater than 99% when approximately 5 ppm of HCl was added to the simulated flue gas. Meanwhile, Deacon reaction evaluation and in situ diffuse reflectance infrared Fourier transform (DRIFT) technique were performed for the possible reaction mechanisms.

1. Introduction

As one of the most toxic and volatile heavy metal pollutants, excessive emissions of mercury into the atmosphere are of concern world-wide [1,2]. Thus, an international treaty (the *Minamata Convention on Mercury*) regarding mercury pollution was officially

* Corresponding authors. Tel./fax: +86 21 54745591.
E-mail addresses: nqyan@sjtu.edu.cn (N. Yan), quzan@sjtu.edu.cn (Z. Qu).

http://dx.doi.org/10.1016/j.fuel.2014.04.086
0016-2361/

signed in October, 2013 [3]. Coal-fired power plants are the major anthropogenic mercury emission sources in China and the United States due to their huge coal-based energy consumption. Mercury in coal-fired flue gas is generally present in the three forms: elemental mercury (Hg^0), gaseous oxidized mercury (Hg^{2+}) and particulate-bound mercury (Hg^P). The occurrence of these forms mainly depends on the chlorine content of the coal and combustion conditions [4]. Most of the oxidized and particulate-bound mercury can be readily removed with typical air pollution control devices (APCDs). For example, Hg^P can be captured with fly ash particles by particulate control devices, such as electrostatic precipitators or baghouses. Water-soluble Hg^{2+} can be efficiently removed by installing wet flue gas desulfurization equipment [4,5]. However, because of its high volatility and low solubility, Hg^0 is the dominant mercury species that escapes into the atmosphere from APCDs. Therefore, the conversion of Hg^0 to Hg^{2+} is helpful to obtain greater mercury capture efficiency with the available APCDs [4,6,7]. Many attempts involving catalysts have been investigated to achieve this conversion [8]. For example, the catalysts involved in selective catalytic reduction (SCR) of NO_x process were investigated as potential Hg^0 conversion catalysts when sufficient HCl was present in the flue gas [4,9]. However, it was observed that the conventional SCR catalysts were not effective enough for Hg^0 oxidation in flue gas with low HCl concentrations [4]. In addition, the presence of ammonia (NH_3), employed as the SCR reductant, can significantly inhibit Hg^0 oxidation relative to conventional SCR catalysts [9,10]. Therefore, the oxidation of Hg^0 mainly occurs at the tail section of the SCR unit, which has low NH_3 concentrations.

Meanwhile, the unreacted ammonia slip from SCR units has always been a concern. Because slip ammonia can cause a dust plug in the downstream air-preheater and form secondary fine particulates once it escapes into the atmosphere, it has been regarded as a more sensitive air pollutant than NO_x. Therefore, it has been tentatively regulated to be less 3 ppm for the slip ammonia in China [11]. In many SCR cases (especially for the aged SCR catalysts), the slip ammonia has been found to increased dramatically with a higher stoichiometric ratio of NH_3–NO_x (e.g., >0.9).

In this study, we present a novel SCR-Plus catalyst concept, which will work like a typical SCR catalyst for NO_x reduction but will also further convert Hg^0 and unreacted ammonia. To obtain optimal results, the SCR-Plus catalyst can cooperate with a typical SCR catalyst, as suggested in Fig. 1. In this case, a section of the SCR-Plus is set only approximately 1/8–1/4 of the total SCR unit length. Therefore, the SCR-Plus catalyst should perform at a high space velocity.

Our previous study indicated that the ruthenium (Ru) modified SCR catalyst had a high catalytic activity for Hg^0 oxidation with low HCl concentrations [12]. However, the effect of Ru in the SCR catalyst on the conversion of slip ammonia is not clear yet. Moreover, Ru is usually considered as a noble metal and is more expensive than most of the transition metals. Thus, molybdenum (Mo) which was found to have cooperative effect with Ru and would modify the electronic properties of nearby Ru atoms [13,14], was employed to try to enhance the performance of the SCR-Plus catalyst while using lower Ru concentrations. The NO_x reduction, the oxidation of Hg^0 and the abatement of NH_3 were investigated with the SCR-Plus catalysts. In addition, the Hg^0 and ammonia conversion mechanisms were discussed.

2. Experimental

2.1. Materials and catalyst preparations

Commercial TiO_2 (standard Degussa P25) powder, which contains anatase and rutile phases at a ratio of approximately 3:1, was used as a carrier for the various catalysts. All chemicals used for the preparation of catalysts were of analytical grade and purchased from Sigma–Aldrich Co. or Sino-pharm Chemical Reagent Co. The SO_2, NH_3, NO_x, and HCl gases were supplied by Dalian Date Gas Co.

Several *SCR-Plus* catalysts, including the Ru/SCR and Mo–Ru/SCR catalysts, were investigated. The stoichiometric ratios of the Ru oxides to TiO_2 were set at approximately 0.2% or 1% for the Ru/SCR. And for Mo–Ru/SCR catalysts, the Ru and Mo oxide content to TiO_2 was set at 0.2% and 1%, respectively. A self-made TiO_2 based SCR catalyst that consisted of 5% WO_3 and 0.5% V_2O_5 was used as the reference catalyst and as a carrier for the other modified catalysts. The catalysts were all prepared by the wet impregnation methods (Appendices).

2.2. Catalytic activity measurement

The elemental mercury oxidation test system consisted of a permeation tube of Hg^0, a fixed-bed reactor, a cold vapor atomic absorption spectrometer which calibrated by Lumex RA915+ and an online data acquisition system (Fig. A1). The stable air with a given elemental mercury concentration flowed through the blank tube and the reactor tube to provide mercury signals. Catalyst particles (40–60 mesh particles) were placed in the reactor with quartz wool under atmospheric pressure and at controlled temperatures. Generally, the space velocity for the laboratory tests with SCR catalyst particles was between 5.0×10^4 and $1.5 \times 10^5\ h^{-1}$ [15], which was greater than that of the actual SCR operation ($4000–8000\ h^{-1}$) due to the catalyst configuration difference (e.g., small particles *vs.* honeycomb). Considering that the length of the SCR-Plus was set only 1/8–1/4 that of the SCR units, the space velocity across the SCR-Plus section should be 4–8 times greater than in the SCR operation. Thus the space velocities of the SCR-Plus catalyst tests were set at 1.0×10^5–$5.9 \times 10^5\ h^{-1}$, which corresponded to a gas flow rate of 30 L/h with 30–180 mg of catalysts.

The inlet elemental mercury concentration in the gas was controlled at approximately 200 (±10) $\mu g/m^3$, which was greater than that in the actual flue gas (<40 $\mu g/m^3$). However, this high concentration was helpful to shorten the initial adsorption time and to minimize the relative error due to continuous data acquisition in the tests.

In addition, the catalytic activity of the catalysts was also evaluated based on Deacon reaction evaluation unit (chlorine yield as the marker). The Cl_2 concentration in the outlet was monitored a UV/vis spectrometer (BWTEK BRC642E, USA) assorted by a self-made photo cell with 80 cm of the optical length. Meanwhile, detector tube (GASTEC No. 8La) method was used to determine the low level of Cl_2. NH_3, NO, NO_2 and N_2O concentrations were continually monitored with FTIR Multigas analyzer (IMACC, E-3200-C) .

2.3. Catalyst characterization

X-ray diffraction (XRD) measurements were conducted with a diffractometer (D/max2200/PC, Rigaku, Japan) with Cu Kα radiation to determine the distribution of crystalline species in the catalysts. The scanning range was from 10 to 80 degrees and the scanning velocity was 7 degrees min^{-1}. X-ray photoelectron spectroscopy (XPS, Thermo ESCALAB 250) measurements were conducted with Al Kα radiation as the excitation source. Transmission electron microscopy (TEM) was used to investigate the catalyst microstructures with an electron microscope (JEM-2010, JEOL, Japan). The H_2 temperature program reduction (H_2-TPR) curves were conducted with chemisorption analyzer (2920, AutoChem II, Micromeritics). The H_2 flow rate was 50 cm^3/min and the temperature ramp rate was 10 °C/min. The in situ diffuse reflectance infrared Fourier transform (DRIFT) spectroscopy were

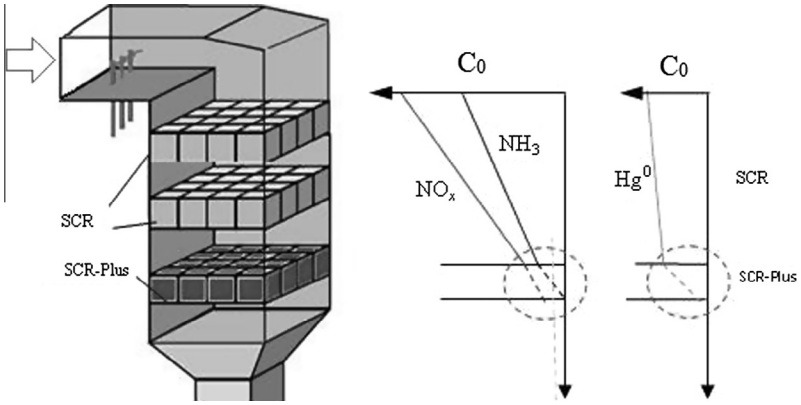

Fig. 1. The conception of the SCR-Plus and its integration with the typical SCR catalyst.

recorded on a Fourier transform infrared spectrometer (FTIR, Nicolet 6700).

3. Results and discussion

3.1. Characterization of the catalysts

Various catalysts were prepared in our research, so the characterization of the catalysts should be studied. First, XRD patterns (Fig. A2) of the prepared catalysts were collected that corresponded with the standard anatase (JCPDS:04-0477) and rutile patterns (JCPDS:65-0190). However, MoO_x and RuO_2 were not clearly identified in the diffraction patterns because they were present in low concentrations and were well dispersed on the catalysts. According to the TEM images, the sizes of the catalyst particles were between 20 and 50 nm (Fig. A3).

In addition, the surface information of various catalysts was analyzed by XPS (Fig. A4). The XPS spectra over the spectral regions of Ru 3d, O 1s, Ti 2p, V 2p, W 4f and Mo 3d were evaluated. The Mo binding energies were centered at approximately 235.4 and 232.1 eV, which were assigned to MoO_3 in the Mo modified catalyst [16]. The Ru peaks were centered at approximately 284.6 and 280.7 eV and were very weak due to the low Ru concentrations. These peaks were assigned to RuO_2 [17].

The Hg peaks were centered at approximately 101.3, 105.5 eV and was assigned to Hg^{2+} [18]. The weak Hg and Cl peaks suggested that the elemental mercury was mainly oxidized to Hg^{2+} and was removed in the form of $HgCl_2$. The S 2p peaks were observed in the 0.2%Ru/SCR catalyst sample after experiment with 500 ppm SO_2. The binding energies were mainly centered at approximately 169 and 168.6 eV and were assigned to sulfate (SO_4^{2-}) [19]. However, no obvious S 2p peaks were present in the 1%Mo–0.2%Ru/SCR catalyst sample spectra. These XPS spectra indicates that the doping of Mo could prevent catalyst to be sulfated and enhance the SO_2 tolerance.

3.2. NO reduction performance in the presence of Ru

Since the DeNOx is one of the function of the SCR-Plus, NO reduction performance was evaluated. According to our previous study, the RuO_2 doped SCR catalysts (Ru/SCR) were able to significantly promote Hg^0 oxidation. However, the effect of the Ru in the catalysts on the NO reduction performance remains unclear. Fig. 2 shows the temperature dependency of the NO reduction efficiency and the N_2 selectivity over the various catalysts. Compared with the conventional SCR catalyst, the Ru/SCR catalysts resulted in higher NO reduction activities when the temperature was less than 300 °C. However, the NO reduction efficiency tended to decrease as the temperature continued to increase, especially for the catalyst with 1.0% Ru. Apparently, the Ru in SCR catalyst was helpful for improving the low-temperature catalytic activity for the NO reduction reaction. However, Ru can also decrease NO reduction at higher temperature through other reactions. Among these reactions, it was hypothesized that the rapid decomposition of the reductant (ammonia) in the presence of Ru was the main reason for the lower NO reduction efficiency (discussed later).

$$4NO + 4NH_3 + O_2 \rightarrow 4N_2 + 6H_2O \quad (1)$$

Meanwhile, the selectivity of the N_2 from NO reduction and NH_3 decomposition remained high for the Ru/SCR catalysts and was even higher than that of the SCR at 400 °C in spite of the lower NO reduction efficiency. The nitrogen balance in the gas can be evaluated. Most of the reduced NO and consumed NH_3 that was converted to N_2 and N_2O in the gas was very low. These results indicated that the reaction that resulted in the formation of N_2O was nearly negligible.

3.3. Catalytic activity for Hg^0 over various catalysts

The catalytic oxidation efficiencies of the modified Ru/SCR catalysts on Hg^0 were tested and evaluated under various conditions as shown in Fig. 3. The results showed that the catalyst with 1% doped Ru had very high catalytic activity for Hg^0 oxidation

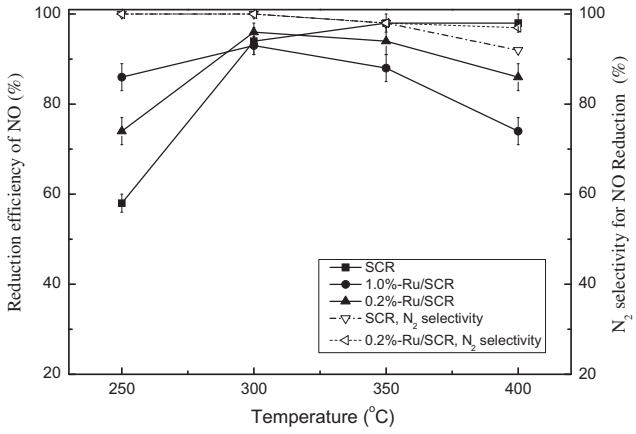

Fig. 2. The NO reduction efficiencies and the N_2 selectivity relative to that of the common SCR catalysts and the Ru modified SCR catalysts. The concentration of NO and NH_3 in the gas was 500 ppm. The gas contains 4% O_2 and N_2. The space velocity (SV) was approximately 35,400 h^{-1}.

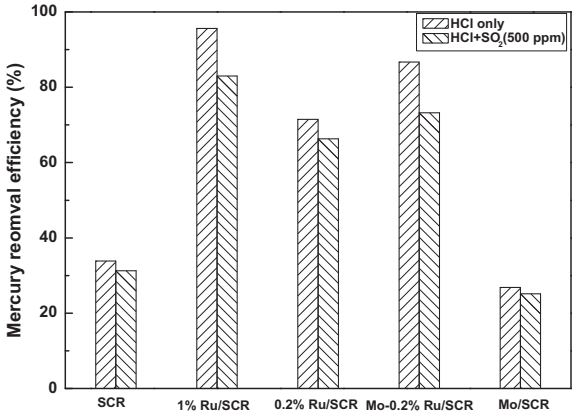

Fig. 3. A comparison of the Hg^0 catalytic oxidation with various catalysts and with 5 ppm HCl and 500 ppm SO_2. The compositions in the gas were 4% O_2 and N_2. The Hg^0 concentration in the gas was approximately 200 (±10) μg/m^3. The space velocity (SV) was approximately 5.9×10^5 h^{-1}. The temperature was 623 K.

(approximately 95% of the oxidation efficiency with 5 ppm HCl). However, the catalyst with 1% doped Ru caused an obvious decrease in the NO reduction efficiency. In addition, the catalyst modification cost was high. When the doped concentration was 0.2%, the catalyst displayed an Hg^0 oxidation efficiency of approximately 70%, which was far greater than that of the SCR catalyst (approximately 35%). Meanwhile, the NO reduction efficiency of the catalyst with 0.2% Ru was approximately 90%, which was approximately 20% higher than that of the 1% Ru doped catalyst (Fig. 2). Therefore, the catalyst doped with 0.2% Ru appeared to be optimal for the trade-off among NO reduction, mercury oxidation and cost (approximately 10–15% higher than that of the conventional SCR catalyst in price).

To improve the oxidation efficiency of Hg^0 relative to that of the 0.2% Ru/SCR catalyst, Mo oxide was used to further modify the catalyst. These results are presented in Fig. 3. The Hg^0 oxidation efficiency of the Mo–Ru/SCR catalyst obviously improved (approximately 86%, an increase of 15% relative to the 0.2%Ru/SCR catalyst). In addition, SO_2 negatively affected the Hg^0 oxidation of the various catalysts in the absence of NO and ammonia. Hg^0 oxidation with the Mo–Ru/SCR catalyst was apparently less inhibited by SO_2. For example, the efficiencies of Mo–Ru/SCR in the absence and presence of 500 ppm SO_2 were approximately 77% and 66%, respectively. The SCR catalyst modified only with Mo cannot enhance Hg^0 oxidation significantly. However, the Mo had an excellent synergetic effect with the Ru/SCR catalyst for Hg^0 oxidation and SO_2 tolerance.

Besides SO_2, the effects of other gaseous components on Hg^0 oxidation in the presence of various catalysts were evaluated (Fig. A5). For example, the presence of NH_3 significantly inhibited Hg^0 oxidation by all of the catalysts. NH_3 could strongly compete with Hg^0 for absorption on the catalyst surfaces and inhibit the activation of HCl by the Deacon reaction [9].

Meanwhile, the coexistence of NO and NH_3 could abate the inhibition of Hg^0 oxidation by NH_3. Furthermore, the Hg^0 oxidation efficiency increased from 20% (with 50 ppm NH_3) to 85% when 50 ppm of NO and NH_3 were present. Two mechanisms may exist to explain this result. First, NO can slightly promote Hg^0 oxidation, as observed in our previous studies and other research [9,12,20]. Secondly, NH_3 can be quickly consumed by NO through reaction Eq. (1) by the catalysts, which can minimize the inhibition Hg^0 oxidation by NH_3. Moreover, the Hg^0 oxidation efficiency of the presulfurized Mo–Ru/SCR catalyst was investigated in simulated flue gas. The results showed that presulfurization could slightly lower the Hg^0 oxidation efficiency (from 91% to 88%). In addition, the Hg^0 oxidation efficiency of Mo–Ru/SCR was greater than 95% in the simulated flue gas after preconditioning with SO_2 for 10 h with space velocities of between 1.0×10^5 and 3.0×10^5 h^{-1} (Fig. A6).

3.4. NH_3 oxidation performance

The NH_3 oxidation performance with various catalysts are shown in Fig. 4. The oxidation of NH_3 over the SCR catalyst was very low in the absence of NO_x. However, the NH_3 decomposition efficiency increased dramatically when 0.2% of Ru was added to the SCR catalysts (from approximately 1% for SCR to 45% for 0.2% Ru/SCR, respectively). This result indicated that the NH_3 molecule was more readily activated by the catalysts with Ru. In addition, it was observed that SO_2 inhibited NH_3 decomposition and that the presence of Mo mitigated this inhibition (Fig. 4). Meanwhile, the NH_3 decomposition efficiency obviously decreased after presulfurization.

In addition, the NH_3 decomposition efficiencies in the presence of NO_x over various catalysts are shown in Fig. 4. As predicted, the NH_3 decomposition was remarkably enhanced by NO_x in the presence of the SCR or other catalysts. In the test condition, the decomposition of NH_3 was only approximately 64% over that of the SCR catalyst. Similarly, the NH_3 decomposition was approximately 75% over that of Mo–Ru/SCR catalyst, respectively. Meanwhile, the NO_x reduction efficiencies were monitored synchronously, which resulted in good stoichiometric agreement with the NH_3 decomposition efficiencies in the respective cases.

In addition, the NH_3 decomposition products in the presence of the various catalysts were also determined. In the absence of NO_x, the main detectable products were N_2 and N_2O (Table A1). However, N_2O concentrations of lower than 0.5 ppm were formed with the Ru/SCR or Mo–Ru/SCR catalysts when 30 ppm of NH_3 was decomposed regardless of the presence or absence of NO_x. This result corresponded to a N_2 selectivity of approximately 97%. It was implied that Eq. (2) was the main NH_3 decomposition reaction, which was accompanied by a very weak reaction (Eq. (3)) to form N_2O. Overall, the NH_3 decomposition efficiency over Mo–Ru/SCR in the simulated flue gas after preconditioning under SO_2 for 10 h with space velocities of between 1.0×10^5 and 3.0×10^5 h^{-1} was as high as 95% (Fig. A7).

$$4NH_3 + 3O_2 \rightarrow 2N_2 + 6H_2O \quad (2)$$

$$2NH_3 + 2O_2 \rightarrow N_2O + 3H_2O \quad (3)$$

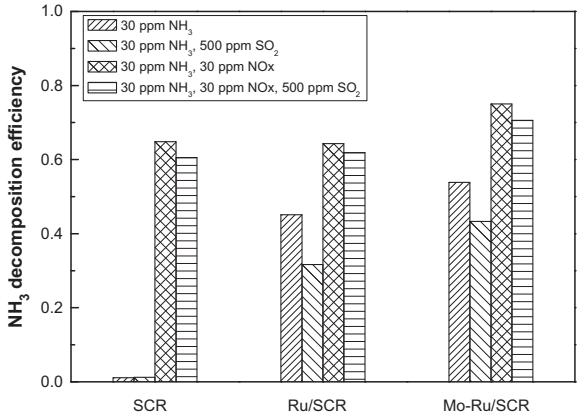

Fig. 4. The NH_3 decomposition efficiencies of the SCR, Ru/SCR and Mo–Ru/SCR catalysts. The space velocity (SV) was approximately 5.9×10^5 h^{-1}. The temperature was 623 K. 30 ppm NH_3: 31.5 ppm; 30 ppm NO_x: 28.96 ppm NO, 0.30 ppm N_2O, 4.25 ppm NO_2. The other gas compositions were 4% O_2 and N_2.

3.5. Determination of HCl activation reaction

In general, the Hg^0 oxidation of the catalysts in the presence of HCl was attributed to the outcome of the Deacon reaction, in which the activation of HCl to form Cl atoms is necessary. Though chlorine has been proven not to be essential for Hg^0 oxidation, it can act as a marker of the catalytic activity because Cl atoms in the catalysts can be further combined with each other to form chlorine. Therefore, the performance of the Deacon reaction and the Hg^0 oxidation of the catalysts can be evaluated with chlorine yield as a marker. In our previous research, the 1%Ru doped SCR catalyst displayed outstanding performance of Cl_2 yield with and without SO_2 [12]. But when the content of Ru decreased to 0.2%, the results were different. As shown in Fig. 5, the Cl_2 yield of the Mo–Ru/SCR catalyst was much higher than that of the SCR and Ru/SCR catalysts with both low and high HCl concentration. This result indicated that the addition of Mo promoted the HCl activation reaction by the Ru/SCR catalyst.

In addition, the production of Cl_2 can be completely inhibited in the presence of all catalysts by a SO_2 concentration of 500 ppm. These results indicated that the production of Cl_2 was very sensitive to SO_2 and that the combination reaction of chlorine atoms to form Cl_2 may be inhibited by SO_2. However, the catalytic oxidation of Hg^0 can still proceed at high efficiencies in such cases (Fig. 3) without yielding chlorine. Therefore, the catalytic oxidation of Hg^0 was mainly dependent on the atomic chlorines which were generated from the abstraction of hydrogen from HCl rather than Cl_2.

According to the HCl activation in the presence of Ru, the unsaturated Ru site (Ru_{cus}) was regarded as the main initiator of HCl activation and the Deacon reaction (reactions (4)–(8), $Ru_{cus-\square}$ means vacant sites on Ru) [21,22]. First, the gaseous oxygen was very easily adsorbed and chemically activated by Ru_{cus} to form active oxygen species of O_{br} (Eq. (4)). The existence of O_{br} over Ru_{cus} would further induce hydrogen abstraction reactions from HCl, which is also the initial step for HCl activation and Cl_2 formation in the Deacon reaction (Eqs. (4)–(8)). According to the results in Fig. 5, it is reasonable to propose that when SO_2 exists, Eq. (7) is stopped but Eq. (8) can continue.

$$2Ru_{cus-\square} + O_2 \rightarrow 2Ru_{cus} - O^* \quad (4)$$

$$Ru_{cus} - O^* + HCl \rightarrow Ru_{cus} - OH - Cl^* \quad (5)$$

$$4Ru_{cus} - OH - Cl^* \rightarrow 4Ru_{cus} - Cl^* + 2H_2O + O_2 \quad (6)$$

$$2Ru_{cus} - Cl^* \rightarrow 2Ru_{cus-\square} + Cl_2 \quad (7)$$

$$2Ru_{cus} - Cl^* + Hg^0 \rightarrow 2Ru_{cus-\square} + HgCl_2 \quad (8)$$

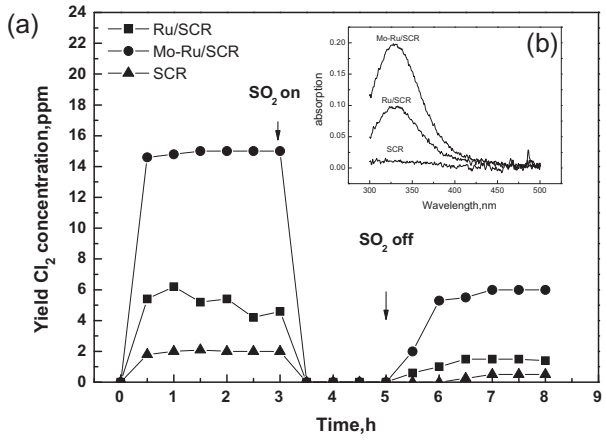

Fig. 5. The Cl_2 concentration produced by the Deacon reaction with the SCR, Ru/SCR and Mo–Ru/SCR catalysts. (a) The HCl concentration in the gas was approximately 280 ppm. The SO_2 concentration in the gas was 500 ppm. The other gas compositions were 4% O_2 and N_2. The space velocity (SV) was approximately 340,000 h^{-1}. The temperature was 623 K. (b) The HCl concentration in the gas was approximately 5000 ppm. The other gas compositions were 4% O_2 and N_2. The space velocity (SV) was approximately 5.9×10^4 h^{-1}. The temperature was 623 K.

3.6. Mechanism of NH_3 decomposition

The mechanism for NH_3 decomposition by Ru/SCR in the presence of O_2 and/or NO is scarcely involved in preceding researches. Therefore, in situ DRIFT was performed to investigate the mechanism of NH_3 decomposition and the results are shown in Fig. 6.

After the adsorption of NH_3 on Ru/SCR at 350 °C, four bands at 1650, 1602, 1415 and 1244 cm^{-1} appeared. The bands at 1650 and 1415 cm^{-1} were assigned to ionic NH_4^+ to the Brønsted acid sites and the bands at 1602 and 1244 cm^{-1} were ascribed to asymmetric and symmetric bending vibrations of the N–H bonds in coordinated NH_3 linked to Lewis acid sites [15,23,24]. After the O_2 passed over the NH_3 pretreated Ru/SCR catalyst, the bands at 1650, 1602, 1415 and 1244 cm^{-1} corresponding to adsorbed ammonia species decreased and vanished within 10 min, which meant that the absorbed ammonia was oxidized by O_2. While with common SCR catalyst, the bands still remained after interaction with O_2 for 40 min (Fig. A9), which also indicated that Ru could facilitated NH_3 oxidation. The results were similar when NO + O_2 passed over the NH_3 pretreated catalysts, only the bands of absorbed NH_3 vanished faster. According to the results of DRIFT

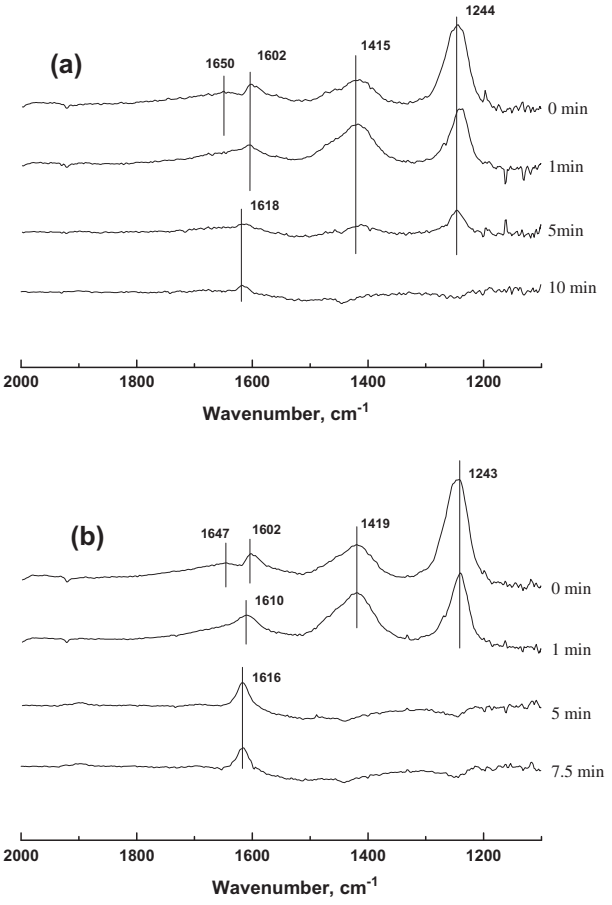

Fig. 6. (a) DRIFT spectra taken at 350 °C upon passing O_2 over the NH_3 presorbed Ru/SCR; (b) DRIFT spectra taken at 350 °C upon passing NO + O_2 over the NH_3 presorbed Ru/SCR.

and Ref. [24], the reaction pathway of NH_3 oxidation over Ru/SCR could be as follow:

$$Ru_{cus} - O^* + NH_3 \rightarrow Ru_{cus} - OH - NH_2 \quad (9)$$

$$2Ru_{cus} - OH - NH_2 \rightarrow 2Ru_{cus} - NH_2^* + H_2O + O^* \quad (10)$$

$$2Ru_{cus} - NH_2^* + O_2 \rightarrow 2Ru_{cus-\square} + N_2 + 2H_2O \quad (11)$$

$$4Ru_{cus} - NH_2^* + 3O_2 \rightarrow 4Ru_{cus-\square} + 2N_2O + 4H_2O \quad (12)$$

$$Ru_{cus} - NH_2^* + O_2 \rightarrow Ru_{cus-\square} + NO + H_2O \quad (13)$$

$$2Ru_{cus} - NH_2^* + 3O_2 \rightarrow 2Ru_{cus-\square} + 2NO_2 + 2H_2O \quad (14)$$

Based on the properties of the main catalyst species, Ru_{cus} and O_{br} should also have played an important role in the NH_3 decomposition process. Hydrogen abstraction from NH_3 by Ru_{cus}–O^* (Eqs. (9) and (10)) should have occurred readily at high temperature [24]. In addition, Ru_{cus}–NH_2^* was potentially an important intermediate species for NH_3 decomposition. In the absence of NO, –NH_2^* would be converted to N_2, N_2O, NO or NO_2 through Eqs. (11)–(14). However, Eqs. (13) and (14) was negligible because few NO and NO_2 were detected. Moreover, the low yield of N_2O (less than 3% of the decomposed NH_3) also indicated that Eq. (12) was not the main reaction. Therefore, Eq. (11) can be regarded as the predominant reaction for NH_3 decomposition in the presence of the Mo–Ru/SCR catalyst. Meanwhile, the significant inhibition of Hg^0 oxidation by NH_3 indicated that Eq. (9) may take precedence over Eq. (8) and/or Eq. (5) when the NH_3 concentration was high.

When NO_x existed, the Ru_{cus}–NH_2^* could react with NO and NO_2 through Eqs. (15) and (16), respectively. In addition, Eqs. (15) and (16) was supposed to be more rapid than that of NH_3 decomposition in the absence of NO_x (Eqs. (11)–(13)) because a greater NH_3 decomposition efficiency can be obtained (Fig. 4).

$$4Ru_{cus} - NH_2^* + 2NO_2 \rightarrow 4Ru_{cus-\square} + 3N_2 + 4H_2O \quad (15)$$

$$Ru_{cus} - NH_2^* + NO \rightarrow Ru_{cus-\square} + N_2 + H_2O \quad (16)$$

3.7. The cooperation of Ru and Mo in the SCR-Plus catalyst

From the above results, it was concluded that the Ru and Mo in the SCR-Plus treatment cooperated well for both Hg^0 oxidation and NH_3 decomposition. The Ru in the catalyst facilitated the oxidation of Hg^0 and NH_3. Generally, Mo was not regarded as the active element, but was found to have cooperative effect with Ru and would modify the electronic properties of nearby Ru atoms [13,14]. Meanwhile, Mo was a good candidate for improving the SO_2 tolerance of the catalysts [25].

To investigate the redox behavior of the catalysts, the temperature program reduction (TPR) by hydrogen for the Ru/SCR and Mo–Ru/SCR catalysts were tested. These results are shown in Fig. A8. In the SCR catalyst, a shoulder peak at 936 °C corresponds to the reduction of W^{6+} and the weak peak at 685 °C corresponds to the reduction of low concentration V^{5+} [26]. What is more, the peak at 206 °C and 235 °C in 1%Ru/SCR corresponds to the reduction of Ru^{4+}, which was assigned to well self-crystallized RuO_2 particles [27]. As for the catalyst 2%Mo–1%Ru/SCR, all the peaks about Ru shifted to higher temperature (e.g., from 206 °C to about 225 °C, from 305 °C to 340 °C in the presence of Mo), which may indicate a cooperation effect between Ru and Mo on the catalysts.

Ru_{cus} has played an important role in the Cl_2 yield and NH_3 decomposition process. The fact that the Cl_2 yield and ammonia decomposition over Mo modified Ru/SCR catalyst was greater indicated that more Ru_{cus} sites were available and/or activated at a greater rate in the presence of Mo. Because Ru on the catalyst surface included Ru_{cus} and non-Ru_{cus}, and the Ru_{cus}/(Ru_{cus} + non-Ru_{cus}) ratio reflected the catalytic activity. The presence of Mo in the catalyst may modify the electronic properties of nearby original non-Ru_{cus} atoms [13,14], which resulted in the formation of more Ru_{cus}. The significant increase in Cl_2 yield by the Mo modified Ru/SCR catalysts could be considered as direct evidence for the above hypothesis. Meanwhile, the presence of Mo could prevent SO_2 from interacting with Ru_{cus}, which resulted better SO_2 tolerance.

4. Conclusion

In conclusion, the Mo doped Ru–SCR catalyst displayed excellent performance for the catalytic conversion of Hg^0. In addition, the SO_2 and NH_3 tolerance in the coal-fired flue with low levels of HCl was excellent. The Ru/SCR that was doped with Mo facilitated the activation of HCl. In addition, this treatment also achieved high NO_x removal and NH_3 decomposition efficiency with excellent N_2 selectivity. Therefore, the Mo-Ru/SCR catalyst appears to have potential for synchronously removing Hg^0 and slip ammonia from industrial coal-fired flue gas.

Acknowledgments

This study was supported by the National Basic Research Program of China (973) under Grant No. 2013CB430005, the NSFC projects (Nos. 21077073 and 21277088) and the National High-Tech R&D Program (863) of China (No. 2013AA065403).

Appendix A. Supplementary material

The XRD patterns, TEM images, H_2-TPR curves and the supplementary data associated with this article can be found, in the online version, at http://dx.doi.org/10.1016/j.fuel.2014.04.086.

References

[1] Pacyna EG, Pacyna JM, Sundseth K, Munthe J, Kindbom K, Wilson S, et al. Global emission of mercury to the atmosphere from anthropogenic sources in 2005 and projections to 2020. Atmos Environ 2010;44:2487–99.
[2] Wu Y, Wang SX, Streets DG, Hao JM, Chan M, Jiang JK. Trends in anthropogenic mercury emissions in China from 1995 to 2003. Environ Sci Technol 2006;40:5312–8.
[3] Mackey TK, Contreras JT, Liang BA. The minamata convention on mercury: attempting to address the global controversy of dental amalgam use and mercury waste disposal. Sci Total Environ 2014;472:125–9.
[4] Presto AA, Granite EJ. Survey of catalysts for oxidation of mercury in flue gas. Environ Sci Technol 2006;40:5601–9.
[5] Zhuang Y, Thompson JS, Zygarlicke CJ, Pavlish JH. Development of a mercury transformation model in coal combustion flue gas. Environ Sci Technol 2004;38:5803–8.
[6] Wang YJ, Liu Y, Wu ZB, Mo JS, Cheng B. Experimental study on the absorption behaviors of gas phase bivalent mercury in Ca-based wet flue gas desulfurization slurry system. J Hazard Mater 2010;183:902–7.
[7] Li X, Lee JY, Heald S. XAFS characterization of mercury captured on cupric chloride-impregnated sorbents. Fuel 2012;93:618–24.
[8] Wang M, Zhu T, Luo H, Wang H, Fan W. Effects of reaction conditions on elemental mercury oxidation in simulated flue gas by DC nonthermal plasma. Ind Eng Chem Res 2011;50:5914–9.
[9] Niksa S, Fujiwara N. A predictive mechanism for mercury oxidation on selective catalytic reduction catalysts under coal-derived flue gas. J Air Waste Manage 2005;55:1866–75.
[10] Senior CL. Oxidation of mercury across selective catalytic reduction catalysts in coal-fired power plants. J Air Waste Manage 2006;56:23–31.
[11] Engineering technical specification of flue gas selective catalytic reduction denitration for thermal power plant. HJ 562-2010, 2010.
[12] Yan NQ, Chen WM, Chen J, Qu Z, Guo YF, Yang SJ, et al. Significance of $RuO_{(2)}$ modified SCR catalyst for elemental mercury oxidation in coal-fired flue gas. Environ Sci Technol 2011;45:5725–30.
[13] Scott C, Betancourt P, Pérez Zurita M, Bohvar C, Goldwasser J. A study of Ru–Mo/Al_2O_3 catalysts. Appl Catal A: Gen 2000;197:23–9.

[14] Vít Z, Gulková D, Kaluža L, Zdražil M. Synergetic effects of Pt and Ru added to Mo/Al_2O_3 sulfide catalyst in simultaneous hydrodesulfurization of thiophene and hydrogenation of cyclohexene. J Catal 2005;232:447–55.
[15] Chen L, Li J, Ge M. DRIFT study on cerium–tungsten/titiania catalyst for selective catalytic reduction of NO_x with NH_3. Environ Sci Technol 2010;44:9590–6.
[16] Song KY, Park MK, Kwon YT, Lee HW, Chung WJ, Lee WI. Preparation of transparent particulate MoO_3/TiO_2 and WO_3/TiO_2 films and their photocatalytic properties. Chem Mater 2001;13:2349–55.
[17] Chu S-Z, Wada K, Inoue S, Hishita SI, Kurashima K. Fabrication and structural characteristics of ordered TiO_2–Ru (–RuO_2) nanorods in porous anodic alumina films on ITO/glass substrate. J Phys Chem B 2003;107:10180–4.
[18] Pan S, Zhang Y, Shen H, Hu M. An intensive study on the magnetic effect of mercapto-functionalized nanomagnetic Fe_3O_4 polymers and their adsorption mechanism for the removal of Hg (II) from aqueous solution. Chem Eng J 2012.
[19] Castaño JG, Arroyave C, Morcillo M. Characterization of atmospheric corrosion products of zinc exposed to SO_2 and NO_2 using XPS and GIXD. J Mater Sci 2007;42:9654–62.
[20] Li HL, Wu CY, Li Y, Zhang JY. $CeO_{(2)}$–$TiO_{(2)}$ catalysts for catalytic oxidation of elemental mercury in low-rank coal combustion flue gas. Environ Sci Technol 2011;45:7394–400.
[21] Over H. Atomic-scale understanding of the HCl oxidation over RuO_2, a novel deacon process. J Phys Chem C 2012;116:6779–92.
[22] Teschner D, Novell-Leruth G, Farra R, Knop-Gericke A, Schlögl R, Szentmiklósi L, et al. In situ surface coverage analysis of RuO_2-catalysed HCl oxidation reveals the entropic origin of compensation in heterogeneous catalysis. Nat Chem 2012;4:739–45.
[23] Jung SM, Grange P. DRIFTS investigation of V=O behavior and its relations with the reactivity of ammonia oxidation and selective catalytic reduction of NO over V_2O_5 catalyst. Appl Catal B: Environ 2002;36:325–32.
[24] Zhang L, He H. Mechanism of selective catalytic oxidation of ammonia to nitrogen over Ag/Al_2O_3. J Catal 2009;268:18–25.
[25] Infantes-Molina A, Merida-Robles J, Rodriguez-Castellon E, Fierro JLG, Jimenez-Lopez A. Effect of molybdenum and tungsten on Co/MSU as hydrogenation catalysts. J Catal 2006;240:258–67.
[26] Chen L, Li J, Ge M. Promotional effect of Ce-doped V_2O_5–WO_3/TiO_2 with low vanadium loadings for selective catalytic reduction of NO_x by NH_3. J Phys Chem C 2009;113:21177–84.
[27] Ma L, He D. Hydrogenolysis of glycerol to propanediols over highly active Ru–Re bimetallic catalysts. Top Catal 2009;52:834–44.